J. Quant. Spectrosc. Radiat. Transfer Vol. 30, No. 2, pp. 143–161, 1983
Printed in Great Britain.

0022–4073/83 $3.00 + .00
Pergamon Press Ltd.

NUMBER OF TERMS REQUIRED IN THE FOURIER EXPANSION OF THE REFLECTION FUNCTION FOR OPTICALLY THICK ATMOSPHERES

MICHAEL D. KING

Laboratory for Atmospheric Sciences, Goddard Space Flight Center, NASA, Greenbelt, MD 20771, U.S.A.

(*Received* 8 *October* 1982)

Abstract—Computational results have been obtained for the separate terms in the Fourier expansion of the reflection function of an optically thick, conservatively scattering, atmosphere composed of cloud particles. The computations were obtained by successive applications of the invariant imbedding, doubling and asymptotic fitting methods to cover the range from very thin to very thick atmospheres. Results are presented which illustrate the magnitude of the separate terms in the Fourier expansion of the phase function and the Fourier expansion of the reflection function of a semi-infinite atmosphere as a function of the zenith angles of incidence and reflection. The azimuthally independent reflection function is enhanced by as much as a factor of 115 over the first-order reflection function, whereas the azimuth-dependent reflection functions generally result from less multiple scattering. These results are compared with those for an atmosphere having a Henyey–Greenstein phase function with the same asymmetry factor ($g = 0.84123$) as in the cloud model. The relative difference in the escape function and azimuthally independent reflection function is generally less than a few per cent, though differences up to 70% occur in the reflection function at angles where single scattering is important. Results are also presented which show the number of terms required in the Fourier expansion of the reflection function to be assured an accuracy of 0.1%. The number of terms required depends strongly on the zenith angles of incidence and reflection as well as on details of the phase function.

1. INTRODUCTION

The scattering of sunlight in planetary atmospheres is often characterized by anisotropic phase functions expressible as finite expansions of Legendre polynomials. For atmospheres composed of particles large compared to the wavelength of the incident light, as in terrestrial clouds at visible wavelengths, this series may consist of up to a few hundred terms. For multiple scattering calculations it is convenient to transform the reference system from the plane of scattering to two vertical planes containing the directions of incidence and scattering. Using the addition theorem for spherical harmonics the phase function is thereby expressible as a Fourier series in the cosine of the azimuthal angle. Though the number of terms required in the Fourier expansion of the phase function may be as many as in the Legendre series at some angles, Dave,[1] Dave and Gazdag,[2] and Herman and Browning[3] have shown that the required number of terms varies substantially with the angles of incidence and scattering.

Regardless of the number of terms required to express the phase function as a Fourier series in the cosine of the azimuthal angle, the maximum number of terms required to describe the reflected and transmitted intensities will not exceed the number of terms required to describe the phase function.[3] This led many authors[2–5] to suggest that multiple scattering computations could be made less time consuming by restricting the computations to a few azimuthal terms. Since the number of terms required to describe the intensity field to a given level of accuracy depends not only on the angles of incidence and scattering but also on the optical thickness of the atmosphere, it is not in general possible to estimate *a priori* the number of azimuthal terms to be carried in the computations.

van de Hulst[6] has presented empirical results for the separate terms in the Fourier expansion of the reflection function of semi-infinite atmospheres. These results, which were based on the analytic phase function first introduced by Henyey and Greenstein,[7] suggest that if either the zenith angle of incidence (θ_0) or reflection (θ) is well removed from the grazing directions, the required number of Fourier terms is small. Furthermore, van de Hulst[6] concludes that the required number of terms varies in accordance with the expression $M(\theta, \theta_0) = 25 \sin \theta_1$, where θ_1 is the smallest of θ and θ_0. Hansen and Travis[5] present selected results for an optically thick atmosphere ($\tau_c = 128$) composed of a polydisperse collection of aerosol particles. In contrast to the results obtained using the Henyey–Greenstein phase function,[6] the Mie theory results of Hansen and Travis[5] show that the required number of terms

may be larger when $\theta = \theta_0$ than when θ is either smaller or larger than θ_0. Their illustration of the separate terms in the Fourier expansion of the reflection function for selected values of θ and θ_0 is noticeably more variable than the comparable Henyey–Greenstein results presented by van de Hulst.[6] Since the separate terms in the Fourier expansion of the reflection function for a Mie theory phase function undergo frequent reversals of sign and since their magnitude decreases less rapidly with increasing order of the Fourier series than does the comparable Henyey–Greenstein results, it appears clear that conclusions drawn for a Henyey–Greenstein phase function may differ from those drawn for a Mie theory phase function.

The intent of this paper is to present computational results for the separate terms in the Fourier expansion of the phase function and the Fourier expansion of the reflection function of a semi-infinite, conservatively scattering, atmosphere composed of cloud particles. From these results we determine the ratio of the total reflection function to the first-order (single scattering) reflection function and the number of terms required to describe the reflection function to an accuracy of 0.1%. These results are compared with similar results obtained for a Henyey–Greenstein phase function having the same asymmetry factor as in the cloud model.

2. LEGENDRE EXPANSION OF THE PHASE FUNCTION

In many radiative transfer applications it is convenient to express the product of the single scattering albedo ω_0 and the phase function $\Phi(\cos\Theta)$ as a finite expansion in Legendre polynomials of the form

$$\omega_0\Phi(\cos\Theta) = \sum_{l=0}^{L} \omega_l P_l(\cos\Theta), \tag{1}$$

where Θ is the scattering angle and $P_l(\cos\Theta)$ a Legendre polynomial of order l. As a consequence of the orthogonality of the Legendre polynomials, the $L+1$ coefficients ω_l may formally be obtained from

$$\omega_l = \frac{(2l+1)}{2}\omega_0 \int_{-1}^{1} \Phi(\cos\Theta)\, P_l(\cos\Theta)\, \mathrm{d}(\cos\Theta). \tag{2}$$

With these definitions, the phase function satisfies the normalization condition

$$\frac{1}{2}\int_{-1}^{1} \Phi(\cos\Theta)\, \mathrm{d}(\cos\Theta) = 1, \tag{3}$$

with the asymmetry factor g related to the Legendre coefficient ω_1 by

$$\frac{1}{2}\int_{-1}^{1} \Phi(\cos\Theta)\cos\Theta\, \mathrm{d}(\cos\Theta) = g = \omega_1/(3\omega_0). \tag{4}$$

We employ two phase functions in calculations of the reflection function of optically thick atmospheres. The first is a Mie phase function for a wavelength 0.754 μm, refractive index 1.333, and a size distribution of particles of a given radius proportional to $r^6 \exp(-1.6187r)$, where r is the particle radius in μm. This distribution of particles is a gamma distribution with effective radius 5.56 μm, effective variance 0.111, and an asymmetry factor 0.84123. This phase function, illustrated in Fig. 1, is typical of fair weather cumulus (FWC) clouds in the visible wavelength region (see Hansen[8]). The second phase function is the widely used analytic phase function first introduced by Henyey and Greenstein[7] and given by

$$\Phi(\cos\Theta) = (1-g^2)/(1+g^2-2g\cos\Theta)^{3/2}. \tag{5}$$

This function is illustrated in Fig. 1 for the same asymmetry factor as in the FWC model. Though it lacks the structure of the Mie phase function, especially the rainbow and glory features apparent in Fig. 1, its extensive use in radiative transfer modeling studies makes it a valuable phase function with which to compare results obtained with the FWC model.

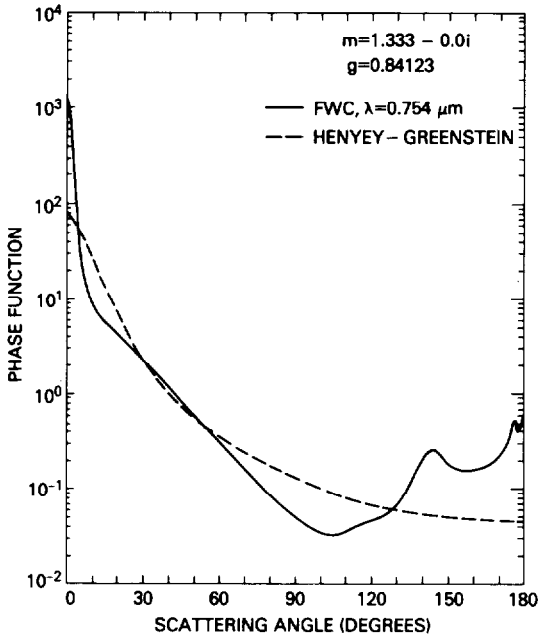

Fig. 1. Phase function as a function of scattering angle for a fair weather cumulus (FWC) size distribution given by $n(r) \alpha r^6 \exp(-1.6187r)$, where $\lambda = 0.754\,\mu$m and $m = 1.333 - 0.0i$. Also shown is the Henyey–Greenstein phase function for the same asymmetry factor as in the FWC model.

One of the features of the Henyey–Greenstein phase function which makes it especially attractive for radiative transfer applications is the simple expression which results for the Legendre coefficients,

$$\omega_l = (2l+1)g^l\omega_0. \tag{6}$$

For a general Mie phase function, no such relationship exists.

Dave[1] and Kattawar *et al.*[9] present formulas for calculating the coefficients of the Legendre series expansion of a Mie phase function for a given size parameter and refractive index. These modified Mie expressions are far more tedious to compute than the well-known Mie expressions for the phase function, due primarily to the fact that the expressions for the Legendre coefficients involve infinite series imbedded within infinite series. As an alternative to using these expressions for hundreds of particle sizes and subsequently integrating over a size distribution, it is sufficient to evaluate the $L+1$ coefficients by numerically integrating over the phase function computed at very small angular intervals. Kattawar[10] evaluated the Legendre coefficients by both methods and found "excellent agreement", though no details were provided on either the quadrature formula used to evaluate the integrals in Eq. (2) or on the difference in computational time between the methods.

In the present investigation, we adopt the quadrature formula

$$\omega_l \approx \frac{(2l+1)}{2}\,\omega_0 \sum_{j=1}^{J} \Phi(\mu_j)\, P_l(\mu_j) c_j, \tag{7}$$

where μ_j are the abscissas and c_j the weights for Gaussian quadrature on the interval $[-1, 1]$. With the phase function a polynomial of degree L, the integrand in Eq. (2) is at most a polynomial of degree $2L$. Since Gaussian quadrature is exact for polynomials of degree less than $2J$, it is essential that the order of the quadrature formula (J) exceed the number of significant Legendre coefficients (L) in the phase function, a number which is not known *a priori*.

Figure 2 illustrates the variation of the coefficients of the Legendre polynomial expansion of the FWC and Henyey–Greenstein phase functions illustrated in Fig. 1. The abscissas and

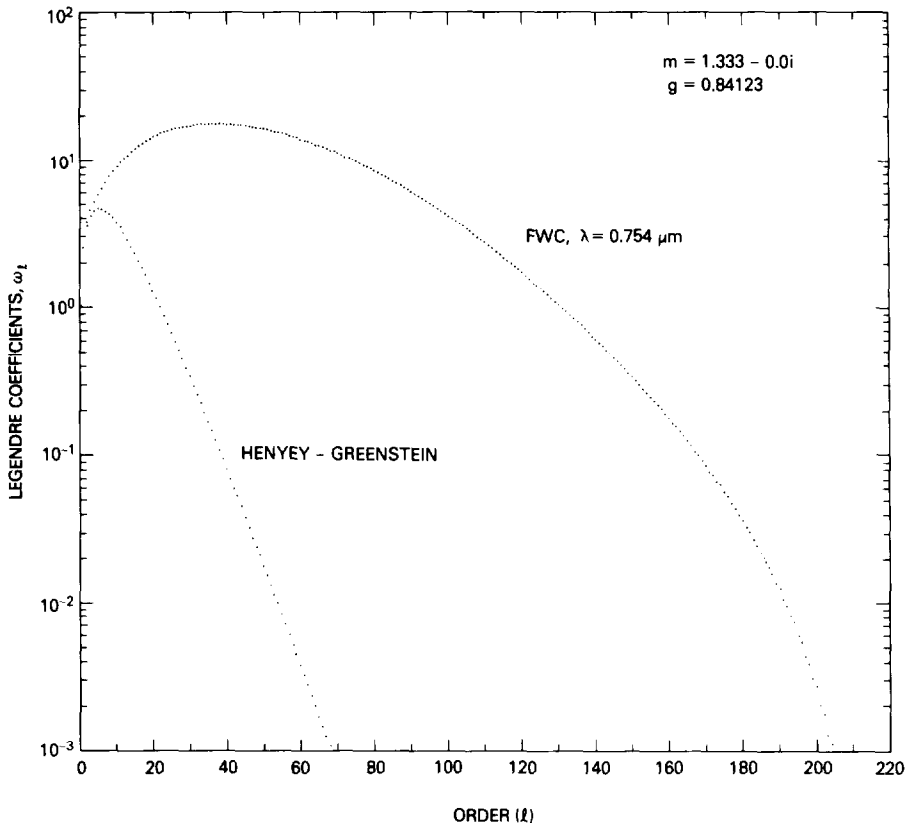

Fig. 2. Coefficients of the Legendre polynomial expansion of the FWC and Henyey–Greenstein phase functions illustrated in Fig. 1.

weights used in evaluating Eq. (7) for the FWC model were taken from Stroud and Secrest[11] for a Gaussian quadrature of order $J = 512$. This results in the first few scattering angles being 0.27°, 0.62°, 0.97° and 1.32°. Based on the somewhat arbitrary criterion that $\omega_l < 10^{-9}\,\omega_0$ for $l > L$, we find that the Legendre expansions are of length $L \approx 152$ for the Henyey–Greenstein model and $L \approx 229$ for the FWC model.

The use of Eq. (7) has several built in accuracy checks. These include the necessity that ω_0 equal the single scattering albedo (unity in the present investigation), that $\omega_1 = 3g\omega_0$, where g is computed directly from the Mie theory, and that the values of the phase function reconstructed from the $L+1$ term Legendre series agree with the values computed from Mie theory. All of these tests were met to an accuracy of at least six significant figures. Though some authors[12-13] recommend using Lobatto quadrature, rather than Gaussian quadrature, in order to include 0° and 180° as explicit quadrature points, we found this to be unnecessary. The time required to evaluate the phase function at 512 scattering angles and at 500 particle sizes, to integrate the phase function over a particle size distribution, and to evaluate the Legendre coefficients was 5.42 min on an IBM 360/91 computer.

3. FOURIER EXPANSION OF THE PHASE FUNCTION

For multiple scattering calculations it is necessary to transform the reference system from the plane of scattering to two vertical planes containing the directions of incidence and scattering. Using the addition theorem for spherical harmonics we obtain the well-known expression[6, 14]

$$\omega_0\Phi(\cos\Theta) = h^0(u, v) + 2\sum_{m=1}^{L} h^m(u, v)\cos m\phi, \tag{8}$$

where the azimuth-dependent redistribution functions $h^m(u, v)$ are given by

$$h^m(u, v) = \sum_{l=m}^{L} \omega_l Y_l^m(u) Y_l^m(v). \tag{9}$$

In these expressions u and v are cosines of the zenith angles of scattering and incidence with respect to the downward normal ($-1 \leq u, v \leq 1$), $Y_l^m(u)$ the renormalized associated Legendre polynomials expressible in terms of the associated Legendre polynomials $P_l^m(u)$ by[15]

$$Y_l^m(u) = \left[\frac{(l-m)!}{(l+m)!}\right]^{1/2} P_l^m(u), \tag{10}$$

and

$$\cos\Theta = uv + (1-u^2)^{1/2}(1-v^2)^{1/2}\cos\phi. \tag{11}$$

Figure 3 illustrates the azimuthally independent redistribution function for reflection, $h^0(-\mu, \mu_0)$, where μ_0 is the cosine of the solar zenith angle and μ the cosine of the zenith angle of reflection with respect to the outward normal ($0 \leq \mu, \mu_0 \leq 1$). The redistribution function for the FWC model is shown in the left portion of the figure while the corresponding function for the Henyey–Grenstein phase function is shown in the right portion. Since $h^0(-\mu, \mu_0)$ represents the product of the single scattering albedo and phase function averaged over azimuth, the values of $h^0(-\mu, \mu_0)$ for $\mu = 1$ or $\mu_0 = 1$ equal those of the phase function itself. The prominent maxima and minima in the backward hemisphere of the FWC phase function (see Fig. 1) lead directly to corresponding features in the redistribution function. For example, the minimum value of $h^0(-\mu, 1)$ at $\mu = 0.264$ corresponds to the minimum of the phase function at $\Theta = 105.3°$, whereas the maxima at $\mu = 0.812$, 0.998 and 1.0 correspond to the rainbow and glory features apparent in Fig. 1. Values of $h^0(-\mu, \mu_0)$ along the diagonal $\mu = \mu_0$ represent averages of the phase function over the range of scattering angles $180° - 2\theta_0 \leq \Theta \leq 180°$, where $\theta_0 = \cos^{-1}\mu_0$. Thus the broad minimum at $\mu = \mu_0 \approx 0.7$ for the FWC model is associated with the broad minimum in the phase function at $\Theta = 105.3°$. For the Henyey–Greenstein phase function, the redistribution function lacks any maxima or minima since the phase function itself is a monotonically decreasing function as the scattering angle increases. In fact the azimuthally independent redistribution function for the Henyey–Greenstein phase function can be expres-

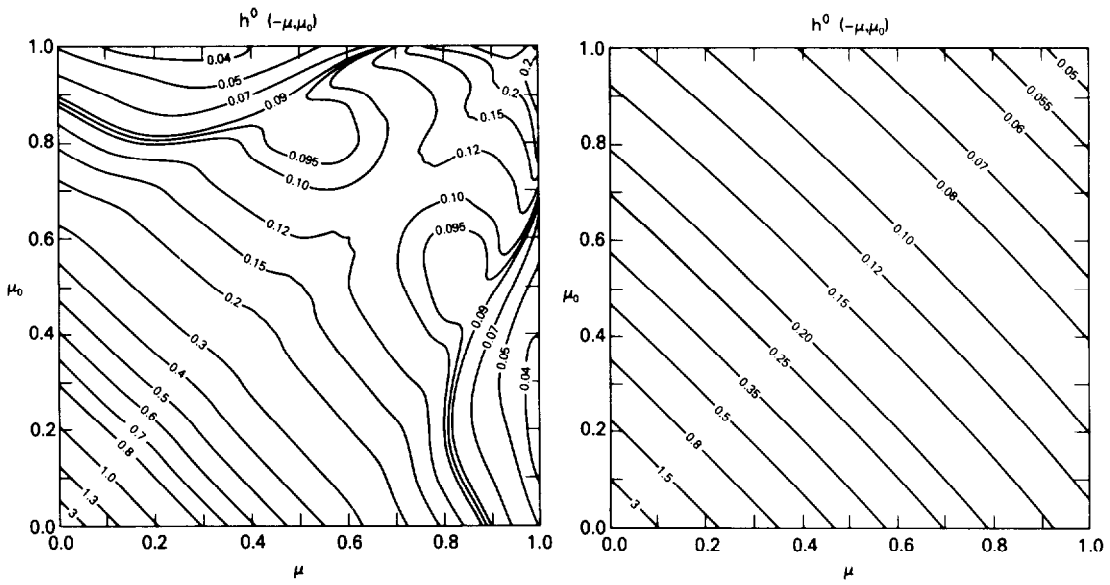

Fig. 3. Azimuthally independent redistribution function for reflection, $h^0(-\mu, \mu_0)$, where the figure on the left applies to the FWC model and the figure on the right to the Henyey–Greenstein model.

sed in terms of the complete elliptic integral of the second kind, as noted by Wiscombe[16] and van de Hulst.[6]

Unlike the azimuthally independent term, the azimuth-dependent terms in the Fourier expansion of the phase function may contain negative as well as positive values. Figure 4 illustrates the first azimuth-dependent redistribution function for reflection, $h^1(-\mu, \mu_0)$, where again the left portion of the figure applies to the FWC model and the right portion to the Henyey–Greenstein model. Due to the monotonically decreasing nature of the Henyey–Greenstein phase function, $h^1(-\mu, \mu_0)$ is positive for all values of μ and μ_0. In contrast, the broad minimum in the FWC phase function at $\Theta = 105.3°$ gives rise to large regions where $h^1(-\mu, \mu_0)$ is negative. These regions are denoted by shading in Fig. 4. When either $\mu = 1$ or $\mu_0 = 1$ the azimuth-dependent redistribution functions $h^m(-\mu, \mu_0) = 0$ for all $m \geq 1$. For these special cases it is adequate to terminate the series in Eq. (8) after the first, azimuthally independent, term. This boundary condition is clearly evident in Fig. 4.

Dave and Gazdag[2] noted that Eq. (8) can be rewritten by replacing the fixed upper limit L of the Fourier series representation of the phase function by a variable upper limit $N(u, v)$. By examining the absolute magnitude of $h^m(u, v)$ as a function of m for selected values of u and v, Dave and Gazdag[2] concluded that $N(u, v)$ is a strong function of u and v, that all $L+1$ terms are required only if $u = v = 0$, and that the maximum number of terms required for a fixed angle of incidence is required when either $u = v$ (transmission) or $u = -v$ (reflection). This latter conclusion was found to be a function of size distribution parameters, for the number of terms required in the Fourier expansion of the phase function for a single particle showed no such maxima at $u = v$ and $u = -v$. For a single particle the required number of terms was found to be a maximum when $u = 0$, regardless of the angle of incidence.

4. NORMALIZATION OF THE REDISTRIBUTION FUNCTION

In performing multiple scattering calculations it is convenient to subdivide the angular interval [0, 1] into K Gaussian quadrature points $0 < \mu_1 < \ldots < \mu_K < 1$ with mirror-symmetric points on the interval $[-1, 0]$ for a total of 2K streams. Then, if the Gaussian weights are $c_1, \ldots, c_K$, it follows that

$$\int_{-1}^{1} h^m(u, \mu_j) Y_m{}^m(u)\, du = \int_0^1 [h^m(-\mu, \mu_j) + h^m(\mu, \mu_j)] Y_m{}^m(\mu)\, d\mu$$

$$= \sum_{i=1}^{K} [h^m(-\mu_i, \mu_j) + h^m(\mu_i, \mu_j)] Y_m{}^m(\mu_i) c_i \tag{12}$$

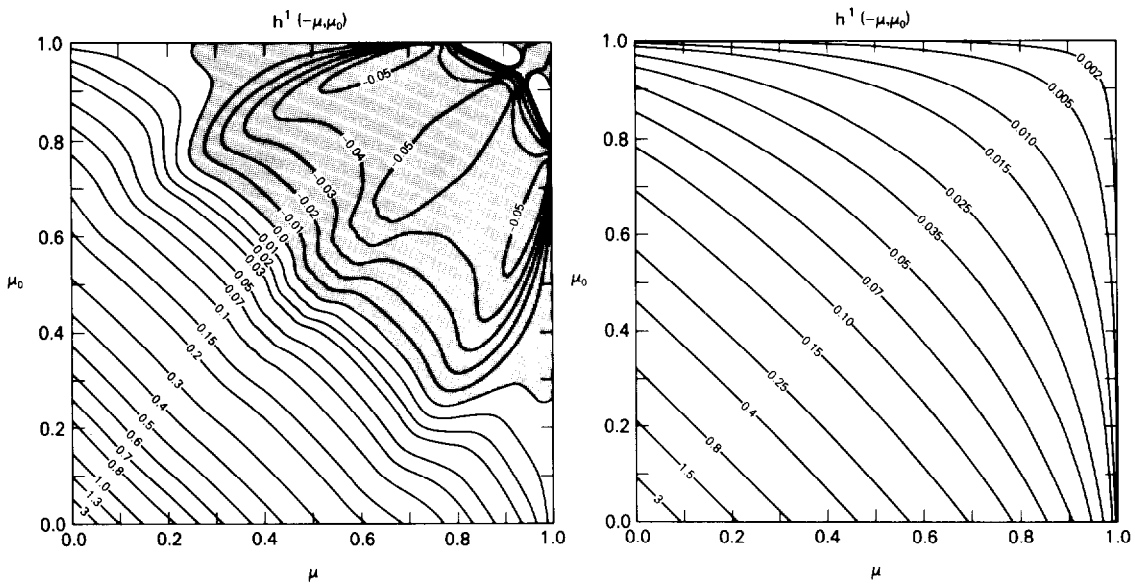

Fig. 4. The same as Fig. 3, except for $h^1(-\mu, \mu_0)$.

for all $j = 1, \ldots, K$. Replacing $h^m(u, \mu_j)$ by its explicit form [Eq. (9)] and noting the orthogonality of the renormalized associated Legendre polynomials, it follows that

$$\int_{-1}^{1} h^m(u, \mu_j) Y_m{}^m(u)\, du = \sum_{l=m}^{L} \omega_l Y_l^m(\mu_j) \int_{-1}^{1} Y_l^m(u) Y_m{}^m(u)\, du$$

$$= \frac{2}{2m+1} \omega_m Y_m{}^m(\mu_j). \tag{13}$$

Combining Eqs. (12) and (13) we find that the phase function must satisfy the following normalization condition in its quadratured form:

$$\sum_{i=1}^{K} [h^m(-\mu_i, \mu_j) + h^m(\mu_i, \mu_j)] Y_m{}^m(\mu_i) c_i = \frac{2}{2m+1} \omega_m Y_m{}^m(\mu_j) \quad (j = 1, \ldots, K). \tag{14}$$

The need to satisfy this equation for the azimuthally independent redistribution function ($m = 0$) has long been recognized in order to conserve flux ($\omega_0 = 1$) or to obtain accurate flux divergence values in multiple scattering calculations.[17] This normalization condition for the azimuth-dependent terms of the redistribution function has not been previously noted in the literature to the author's knowledge. If the phase function is highly asymmetric (large L) and the order of the Gaussian quadrature (K) is too small, Eq. (14) will be poorly satisfied. As a consequence the results of multiple scattering calculations will be inaccurate, especially for optically thick layers with nearly conservative scattering. On the other hand, if K is chosen too large, Eq. (14) and consequently multiple scattering calculations will be highly accurate but enormous amounts of computer time may have been expended. In the doubling method, for example, computer time escalates roughly as K^3 (Hansen[8]) while storage requirements escalate as K^2. This led several investigator's[16–18, 8, 3] to limit the order of their angular discretization and to compensate for the potential loss in accuracy by renormalizing the azimuthally independent redistribution function until Eq. (14) is satisfied. To assure accurate intensity computations as well as accurate flux computations, however, it is equally important that Eq. (14) be satisfied for all $m \geq 0$.

For a fixed angle of incidence the redistribution function is a polynomial of degree L while $Y_m{}^m(\mu)$ is a polynomial of degree m. Since Gaussian quadrature is exact for polynomials of degree less than 2K, a sufficient condition for Eq. (14) to be satisfied is for 2K to exceed $L + m$. Due in part to the small magnitude of the high order Legendre coefficients (see Fig. 2) and in part to the use of Gaussian quadrature on the angular interval [0, 1], we find that Eq. (14) may adequately be satisfied provided

$$K \geq 0.35L. \tag{15}$$

A Gaussian quadrature of order $K = 80$ was used for both the Henyey–Greenstein and FWC models. For the FWC model ($L = 229$) the difference between the left and right sides of Eq. (14) varied from 4.9×10^{-9} to 1.2×10^{-12} for the azimuthally independent term, depending on the direction cosine of the angle of incidence (μ_j). This error decreased with increasing Fourier frequency so that at $m = 30$ the maximum normalization error was 2.1×10^{-15}. Since the same order of angular discretization was used for the Henyey-Greenstein model ($L = 152$), the normalization errors were generally less than for the FWC model. At $m = 0$ the maximum normalization error was 1.9×10^{-14}, reducing to 3.7×10^{-17} at $m = 30$. In no instance was any renormalization performed.

5. FOURIER EXPANSION OF THE REFLECTION FUNCTION

Having determined the azimuth-dependent redistribution functions, multiple scattering calculations were performed to determine the separate terms in the Fourier expansion of the reflection function $R(\tau_c; \mu, \mu_0, \phi)$ and transmission function $T(\tau_c; \mu, \mu_0, \phi)$, where

$$R(\tau_c; \mu, \mu_0, \phi) = R^0(\tau_c; \mu, \mu_0) + 2 \sum_{m=1}^{L} R^m(\tau_c; \mu, \mu_0) \cos m\phi, \tag{16}$$

$$T(\tau_c; \mu, \mu_0, \phi) = T^0(\tau_c; \mu, \mu_0) + 2 \sum_{m=1}^{L} T^m(\tau_c; \mu, \mu_0) \cos m\phi, \tag{17}$$

and τ_c is the total optical thickness of the atmosphere. In terms of these functions, the reflected $I(0, -\mu, \phi)$ and transmitted $I(\tau_c, \mu, \phi)$ intensities from a horizontally homogeneous atmosphere illuminated from above by a parallel beam of radiation of incident flux density F_0 may be expressed in the forms

$$I(0, -\mu, \phi) = (\mu_0 F_0/\pi)\, R(\tau_c; \mu, \mu_0, \phi), \tag{18}$$

$$I(\tau_c, \mu, \phi) = (\mu_0 F_0/\pi)\, T(\tau_c; \mu, \mu_0, \phi). \tag{19}$$

By virtue of the Helmholtz principle of reciprocity each of the azimuth-dependent terms of the reflection and transmission functions is symmetric in μ and μ_0.

The reflection and transmission functions were calculated using the doubling method.[5-6] In this method the reflection and transmission functions of a single layer of optical thickness τ_c are combined with those of a similar layer to obtain the reflection and transmission functions of a combined layer of optical thickness $2\tau_c$. In applying the doubling method it is necessary to obtain the reflection and transmission functions of an initial layer of infinitesimal optical thickness. Many different methods have been used as initializations in the doubling method. Wiscombe[16] described and compared the majority of these methods and concluded that the error in the computational results for most values of the optical thickness can be reduced by many orders of magnitude when the best starting technique is used.

In the present investigation we have solved the integrodifferential equations satisfied by the reflection and transmission functions, known as the principles of invariance, by a second order Runge–Kutta method. Replacing the integrals on the angular interval $[0, 1]$ by a Gaussian quadrature formula with abscissas $0 < \mu_1 < \ldots < \mu_K < 1$ and corresponding weights c_k, the principles of invariance[19] may be written as

$$\begin{aligned}\frac{\partial R^m(\tau_c; \mu, \mu_0)}{\partial \tau_c} &= -\left(\frac{1}{\mu} + \frac{1}{\mu_0}\right) R^m(\tau_c; \mu, \mu_0) + \frac{1}{4\mu\mu_0} h^m(-\mu, \mu_0) \\ &+ \frac{1}{2\mu} \sum_{k=1}^{K} h^m(\mu, \mu_k) R^m(\tau_c; \mu_k, \mu_0) c_k + \frac{1}{2\mu_0} \sum_{k=1}^{K} R^m(\tau_c; \mu, \mu_k) h^m(-\mu_k, -\mu_0) c_k \\ &+ \sum_{k=1}^{K} \sum_{l=1}^{K} R^m(\tau_c; \mu, \mu_k) h^m(-\mu_k, \mu_l) R^m(\tau_c; \mu_l, \mu_0) c_k c_l,\end{aligned} \tag{20}$$

$$\begin{aligned}\frac{\partial T^m(\tau_c; \mu, \mu_0)}{\partial \tau_c} &= -\frac{1}{\mu_0} T^m(\tau_c; \mu, \mu_0) + \frac{1}{4\mu\mu_0} e^{-\tau_c/\mu} h^m(\mu, \mu_0) \\ &+ \frac{1}{2\mu} e^{-\tau_c/\mu} \sum_{k=1}^{K} h^m(-\mu, \mu_k) R^m(\tau_c; \mu_k, \mu_0) c_k + \frac{1}{2\mu_0} \sum_{k=1}^{K} T^m(\tau_c; \mu, \mu_k) h^m(-\mu_k, -\mu_0) c_k \\ &+ \sum_{k=1}^{K} \sum_{l=1}^{K} T^m(\tau_c; \mu, \mu_k) h^m(-\mu_k, \mu_l) R^m(\tau_c; \mu_l, \mu_0) c_k c_l.\end{aligned} \tag{21}$$

Integrating these differential equations from the origin to an optical depth τ_c using a second order Runge–Kutta method[20] we find that the discretized reflection and transmission functions for a thin initial layer may be expressed for all $i, j = 1, \ldots, K$ as

$$\begin{aligned}R^m(\tau_c; \mu_i, \mu_j) &= \frac{\tau_c}{4\mu_i\mu_j}\left[1 - \frac{\tau_c}{2}\left(\frac{1}{\mu_i} + \frac{1}{\mu_j}\right)\right] h^m(-\mu_i, \mu_j) \\ &+ \frac{\tau_c^2}{16\mu_i\mu_j} \sum_{k=1}^{K} [h^m(-\mu_i, \mu_k) h^m(\mu_k, \mu_j) + h^m(-\mu_i, -\mu_k) h^m(-\mu_k, \mu_j)] \frac{c_k}{\mu_k} + O(\tau_c^3),\end{aligned} \tag{22}$$

$$\begin{aligned}T^m(\tau_c; \mu_i, \mu_j) &= \frac{\tau_c}{4\mu_i\mu_j}\left[1 - \frac{\tau_c}{2}\left(\frac{1}{\mu_i} + \frac{1}{\mu_j}\right)\right] h^m(\mu_i, \mu_j) \\ &+ \frac{\tau_c^2}{16\mu_i\mu_j} \sum_{k=1}^{K} [h^m(\mu_i, \mu_k) h^m(\mu_k, \mu_j) + h^m(\mu_i, -\mu_k) h^m(-\mu_k, \mu_j)] \frac{c_k}{\mu_k} + O(\tau_c^3),\end{aligned} \tag{23}$$

where $O(\tau_c^3)$ denotes terms of order τ_c^3 or higher.

Equations equivalent to Eqs. (22) and (23) were derived by Wiscombe[16] by expanding the matrix inversion equations of his diamond initialization in powers of τ_c^3 and retaining terms out to τ_c^2. Wiscombe refers to this method as the expanded diamond initialization, though our derivation from the principles of invariance makes it clear that these equations are equivalent to an invariant imbedding initialization. The first term in each equation represents the contribution from single scattering while the second term represents the contribution from multiple scattering. Equations (22) and (23) are therefore more complex than a single scattering initialization but far less complex than an initialization based on the sum of single plus second order scattering.

Since the computer time required in the invariant imbedding initialization escalates roughly as K^3, as in the doubling method itself, the time required to initialize according to Eqs. (22) and (23) is fixed relative to the time required to perform a single doubling. The diamond initialization recommended by Wiscombe[16] and the fourth order Runge–Kutta method recommended by Kattawar and Plass[21] are both more accurate than the second order Runge–Kutta method presented here, but the computer time required to initialize with these methods escalates roughly as K^4 and K^5, respectively. This makes them less attractive in the absence of phase function renormalization (large K), since the increase in computer time required to initialize the reflection and transmission functions rapidly exceeds the time saved by initializing at a larger initial τ_c.

We have followed Wiscombe's[22] recommendation that the initial layer have an optical thickness $\tau_c \sim \mu_1/100$, where μ_1 is the smallest Gaussian quadrature point. This results in an initial layer of optical thickness 2^{-19}, rather than 2^{-30} as in our earlier work with the single scattering initialization.[23] Since the time required to perform the invariant imbedding initialization is nearly equal to the time required to perform 2 doublings, we reduce the number of doublings required by 11 with a modest increase in the time required to perform the initialization.

In addition to the invariant imbedding and single scattering initializations we performed a limited set of calculations using the diamond initialization with an initial layer of optical thickness 2^{-13} (i.e., $\tau_c \sim \mu_1$). Using the more time consuming diamond initialized doubling results as representative of an exact solution, we compared the reflection and transmission functions, plane albedo and conservation of energy at $\tau_c = 32$ and found in all instances that the invariant imbedding initialized results exceeded in accuracy the single scattering initialized results. Though the single scattering results conserved energy very well, the reflection and transmission functions at most angles of incidence and reflection were less accurate than the invariant imbedding results. This is in agreement with the findings of Kattawar and Plass[21] who showed that the use of energy conservation as a test of accuracy is misleading, for the single scattering initialization conserves energy exactly, except for round-off in the calculations.

When τ_c has been made large enough by the doubling method, the numerical results must agree with known asymptotic expressions for the reflection and transmission functions of very thick layers. In the case of conservative scattering these expressions are given by[24, 6]

$$R(\tau_c; \mu, \mu_0, \phi) = R_\infty(\mu, \mu_0, \phi) - T(\tau_c; \mu, \mu_0, \phi), \tag{24}$$

$$T(\tau_c; \mu, \mu_0, \phi) = 4K(\mu)K(\mu_0)/[3(1-g)(\tau_c + 2q_0)], \tag{25}$$

where $R_\infty(\mu, \mu_0, \phi)$ is the reflection function for a semi-infinite atmosphere, $K(\mu)$ the escape function, and q_0 the extrapolation length for conservative scattering, where $q' = (1-g)q_0$ is known to range between 0.709 and 0.715 for all possible phase functions.[6] Since the transmission function for optically thick layers is azimuthally independent [see Eq. (25)], the entire azimuthal dependence of the reflection function is contained in the Fourier expansion of the reflection function for a semi-infinite atmosphere, given by

$$R_\infty(\mu, \mu_0, \phi) = R_\infty^0(\mu, \mu_0) + 2\sum_{m=1}^{L} R_\infty^m(\mu, \mu_0)\cos m\phi. \tag{26}$$

For the azimuth-independent term of the reflection and transmission functions doubling computations were performed from an initial layer of optical thickness 2^{-19} to a final layer of

optical thickness 32 (24 doublings), from which $R_\infty^0(\mu, \mu_0)$, $K(\mu)$ and q_0 were determined by the asymptotic fitting method of van de Hulst.[24,6] Figure 5 illustrates the escape function $K(\mu)$ as a function of μ for both the FWC and Henyey–Greenstein models. It is evident from this figure that the transmitted radiation at the base of an optically thick atmosphere is 4.86 times greater at the zenith ($\mu = 1$) than at the horizon ($\mu = 0$) for the FWC model (4.33 for the Henyey–Greenstein model). Though the single scattering phase functions differ substantially between these models (see Fig. 1), the relative difference in the escape function is generally less than a few per cent, with the maximum difference of 11% occurring at the horizon.

Once the escape function has been determined, the reduced extrapolation length q' is obtained from the moment integral[6]

$$q' = (1-g)q_0 = 2\int_0^1 K(\mu)\mu^2 \, d\mu, \tag{27}$$

where the integral is evaluated by Gaussian quadrature. The reduced extrapolation length for the FWC model is 0.71478 and for the Henyey–Greenstein model is 0.71394. Since q' shows little sensitivity to details of the phase function, and since $K(\mu)$ must obey the normalization condition

$$1 = 2\int_0^1 K(\mu)\mu \, d\mu, \tag{28}$$

it is not surprising that $K(\mu)$ shows little sensitivity to the high order Legendre coefficients of the phase function.

Figure 6 illustrates the azimuthally independent reflection function for a semi-infinite atmosphere, $R_\infty^0(\mu, \mu_0)$, where the left portion of the figure applies to the FWC model and the right portion to the Henyey–Greenstein model. $R_\infty^0(\mu, \mu_0)$ was determined by applying the asymptotic fitting method[24,6] to doubling computations at an optical thickness of 32, *viz.*, $R_\infty^0(\mu, \mu_0) = R^0(32; \mu, \mu_0) + T^0(32; \mu, \mu_0)$. The difference between the reflected flux density (or plane albedo) of the FWC and Henyey–Greenstein models is generally less than 0.2% at an optical thickness of 32, rising to 0.66% only at grazing incidence. The reflection function

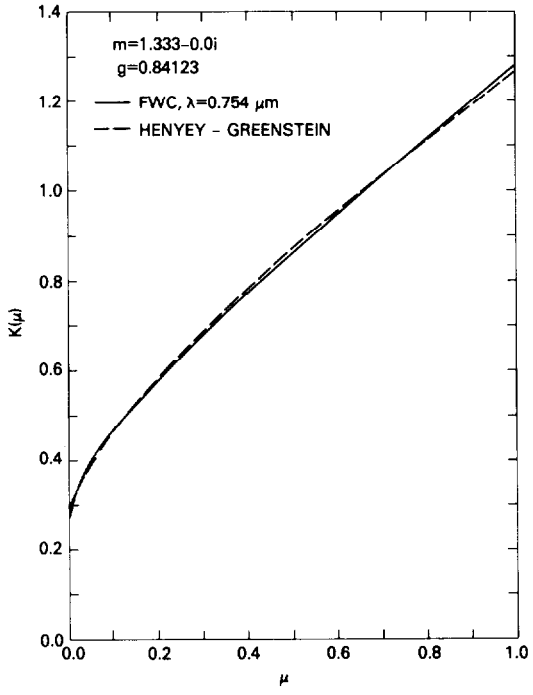

Fig. 5. Comparison of the escape function $K(\mu)$ for the FWC and Henyey–Greenstein models.

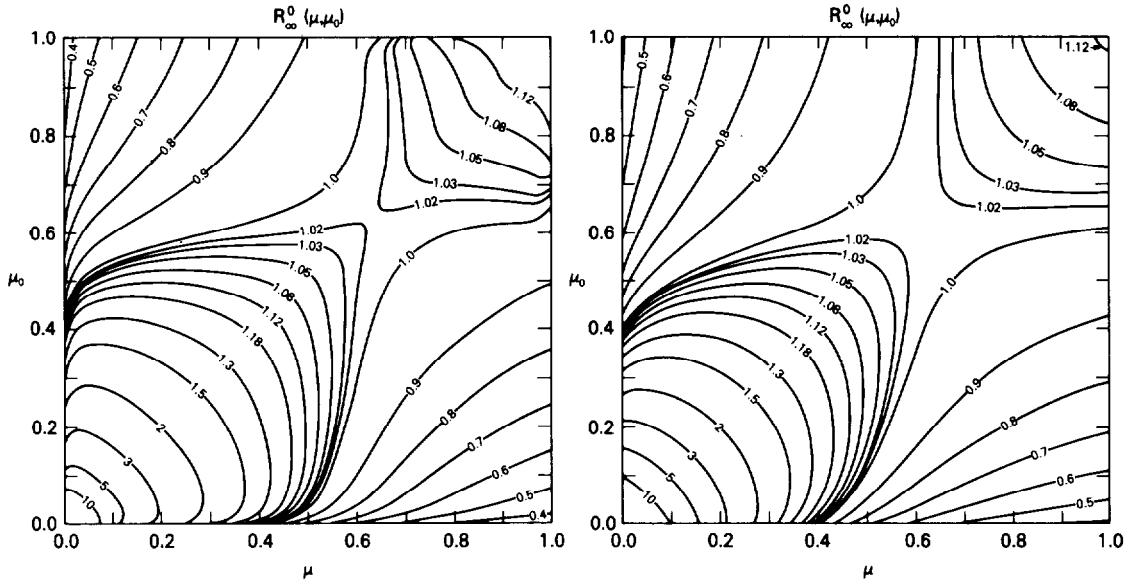

Fig. 6. Azimuthally independent reflection function for a semi-infinite atmosphere, $R_\infty^0(\mu, \mu_0)$, where the figure on the left applies to the FWC model and the figure on the right to the Henyey–Greenstein model.

$R_\infty^0(\mu, \mu_0)$ itself shows differences between the FWC and Henyey–Greenstein models of up to 25% for perpendicular incidence ($\mu_0 = 1$) and 72% for grazing incidence ($\mu_0 = 0$). At some values of μ_0 (*viz.*, $0.30 \lesssim \mu_0 \lesssim 0.35$, $0.63 \lesssim \mu_0 \lesssim 0.74$) the differences in $R_\infty^0(\mu, \mu_0)$ are less than 10% for all values of μ. In general the largest differences in the reflection function occur at angles for which the contribution from multiple scattering is small compared to the contribution from single scattering. Since the reflection function at $\mu = \mu_0 = 0$ is entirely determined by single scattering,[6] the largest difference (72%) occurs at grazing incidence and reflection. For all other values of μ_0 the contribution form multiple scattering is the smallest for grazing reflection, so that the largest difference for a given μ_0 occurs for $\mu \sim 0$.

Combining the results of Figs. 3 and 6, the ratio of the total reflection function to the first-order (single scattering) reflection function may readily be determined. This ratio, given by

$$X_\infty^m(\mu, \mu_0) = 4(\mu + \mu_0)\, R_\infty^m(\mu, \mu_0)/h^m(-\mu, \mu_0), \tag{29}$$

is illustrated in Fig. 7 for the azimuthally independent term ($m = 0$), where again the left portion of the figure applies to the FWC model and the right portion to the Henyey–Greenstein model. It is evident from Fig. 7 that the multiple scattering enhancement factor $X_\infty^0(\mu, \mu_0)$ approaches unity in the limit $\mu = \mu_0 = 0$, as required,[6] and that the smallest multiple scattering enhancement for a given value of μ_0 occurs for $\mu \sim 0$. Furthermore, the enhancement of the first-order reflection function by multiple scattering generally increases as μ and μ_0 increase. Comparing the Henyey–Greenstien results in Figs. 3 and 7 along the diagonal $\mu = \mu_0$, one sees that $h^0(-\mu, \mu_0)$ monotonically decreases as μ increases from 0 to 1, whereas the enhancement of the single scattering reflection function by multiple scattering, as measured by $X_\infty^0(\mu, \mu_0)$, monotonically increases. This trade off gives rise to the well defined saddle point in the reflection function $R_\infty^0(\mu, \mu_0)$ at $\mu = \mu_0 \sim 0.6$ (see Fig. 6).

For the azimuth-dependent terms of the reflection and transmission functions doubling computations were performed from an initial layer of optical thickness 2^{-19} to a final layer of sufficient thickness that the internal and transmitted intensities are negligibly small, as required by Eq. (25). For $1 \leq m \leq 3$ calculations were performed to a final layer of optical thickness 32 (as in the azimuth-independent term). As m increased further it was sufficient to terminate the calculations at an optical thickness of 16 for $4 \leq m \leq 27$ and 8 for $28 \leq m \leq 30$. This necessarily reduced the number of doublings required from 24 ($m \leq 3$) to 22 ($m \geq 28$).

Figure 8 illustrates the azimuth-dependent reflection functions $R_\infty^m(\mu, \mu_0)$ for $m = 1$–4 and for the FWC model. These functions, which are valid for $\tau_c \geq 32$ when $m = 1$–3 and

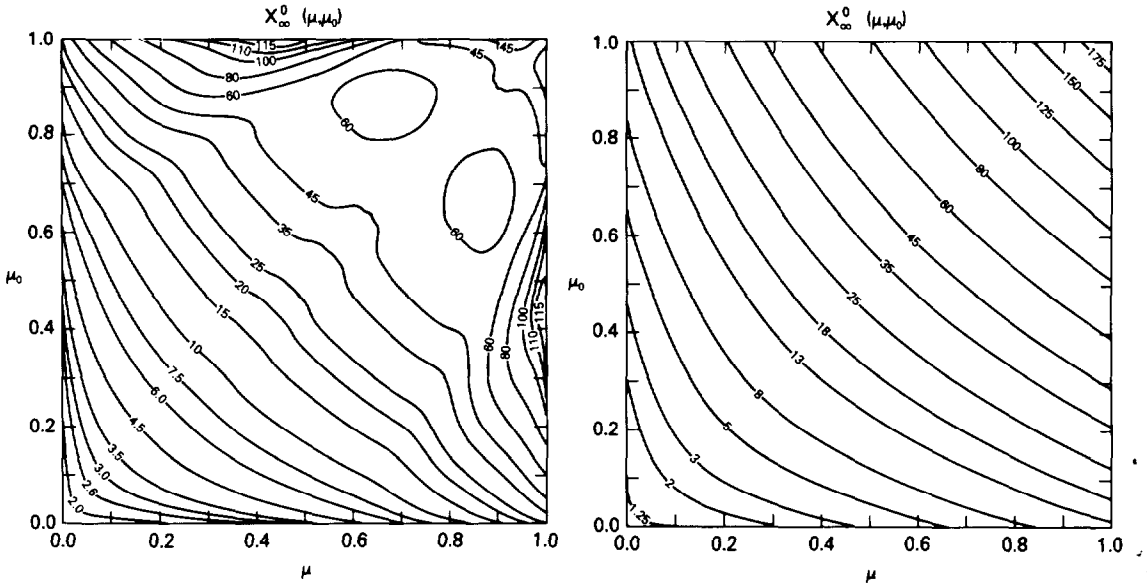

Fig. 7. The same as Fig. 6, except for the ratio of the total reflection function to the first-order (single scattering) reflection function: $X_\infty^m(\mu, \mu_0) = 4(\mu + \mu_0) R_\infty^m(\mu, \mu_0)/h^m(-\mu, \mu_0)$ for $m = 0$.

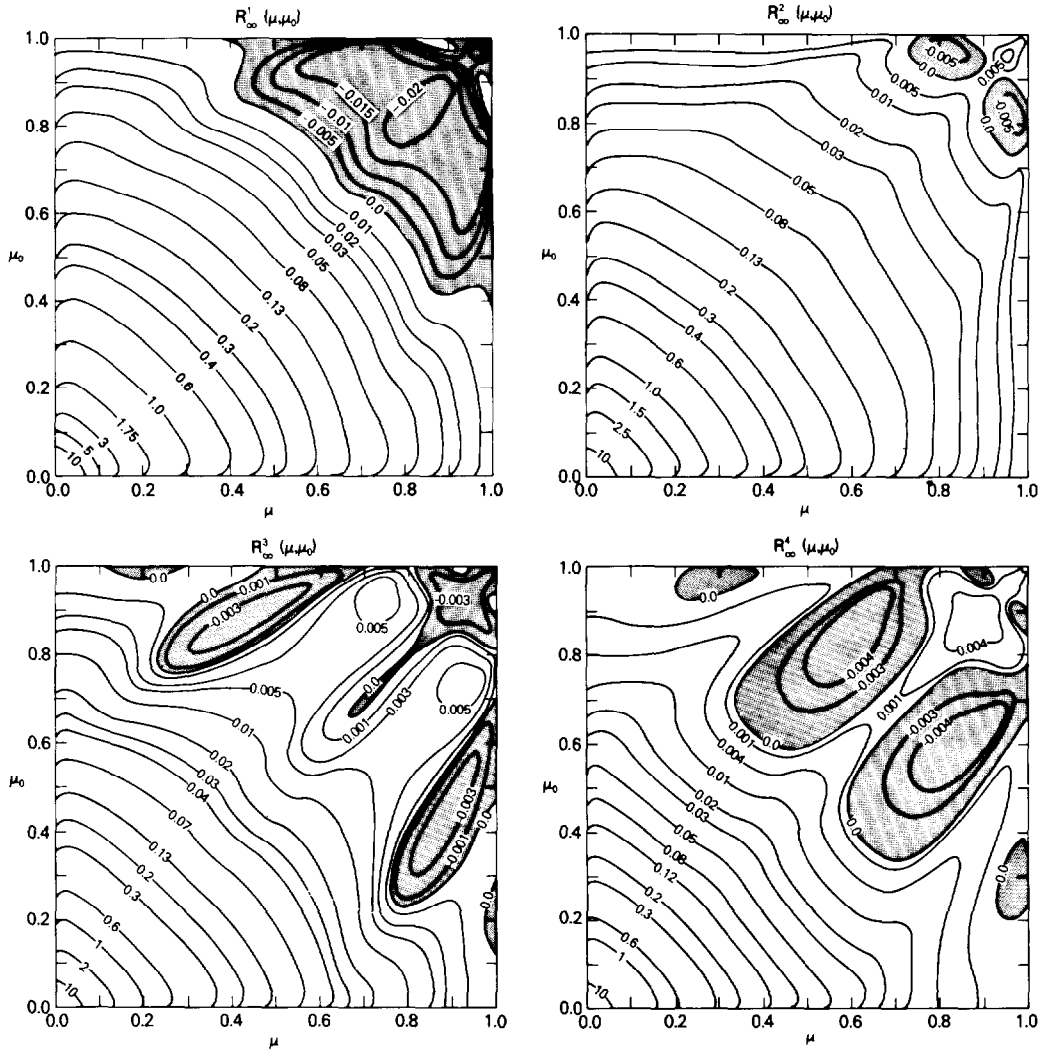

Fig. 8. Azimuth-dependent reflection functions $R_\infty^m(\mu, \mu_0)$ for m = 1–4 and for the FWC model.

$\tau_c \geq 16$ when $m = 4$, necessarily obey symmetry in μ and μ_0, as required by the principle of reciprocity. Comparing the results for $R_\infty^1(\mu, \mu_0)$ with the redistribution function $h^1(-\mu, \mu_0)$, illustrated in Fig. 4, one sees that the distribution of positive and negative values is similar in overall shape but the demarcation between positive and negative values has been shifted in angular position. With the single exception of $R_\infty^2(\mu, \mu_0)$, the reflection functions for increasing Fourier frequency develop an increasing frequency of positive and negative values. At $R_\infty^{30}(\mu, \mu_0)$, for example, nearly half of the angles have negative values for the reflection function, though the absolute magnitude of the reflection function is quite small for the majority of angles.

The azimuth-dependent reflection functions for the Henyey–Greenstein phase function are presented in Fig. 9 for $m = 1$ and 2. The reflection functions for $m = 3$ and 4 (not illustrated) appear similar to those for $m = 1$ and 2, except that the magnitude of $R_\infty^m(\mu, \mu_0)$ as a function of m monotonically decreases for all values of μ and μ_0, especially for μ and μ_0 near 1 (see Section 6). Unlike the FWC results presented in Fig. 8, the azimuth-dependent reflection functions for the Henyey–Greenstein model are positive for all values of μ and μ_0 and for all values of m. Due to azimuthal symmetry when either $\mu = 1$ or $\mu_0 = 1$, it is necessary that $R_\infty^m(\mu, 1) = R_\infty^m(1, \mu_0) = 0$ for all $m \geq 1$. This condition, which is particularly obvious in Fig. 9, is also present in Fig. 8.

As in the case of the azimuth-independent term, it is instructive to examine the ratio of the total reflection function to the first-order reflection function for the $m = 1$ term. This ratio, given by $X_\infty^1(\mu, \mu_0)$, is presented in Fig. 10 for both the FWC (left) and Henyey–Greenstein (right) models. For the Henyey–Greenstein model $X_\infty^1(\mu, \mu_0) \leq X_\infty^0(\mu, \mu_0)$ for all values of μ and μ_0 (see Fig. 7). As m increases further the enhancement of the single scattering reflection function by multiple scattering continues to decrease so that at $m = 3$, $X_\infty^3(\mu, \mu_0)$ is everywhere less than 10.

van de Hulst[25] was the first to observe that the contribution from successive orders of scattering decreases rapidly with increasing order of the Fourier expansion of the reflection function. This led him to suggest that multiple scattering computations might be made less time consuming for large values of m if this observation could be utilized. In addition to the angles of incidence and reflection, however, the azimuth-dependent enhancement factors $X_\infty^m(\mu, \mu_0)$ depend strongly on the details of the phase function, on the single scattering albedo, and on optical thickness. For the Henyey–Greenstein model, for example, the enchancement factor $X_\infty^3(0.5, 0.5) = 5.901$ when $g = 0.84123$. This indicates that higher-order scattering contributes nearly 5 times as much as single scattering to the value of the reflection function at these angles. In contrast, van de Hulst[6] presents results for a conservatively scattering Henyey–

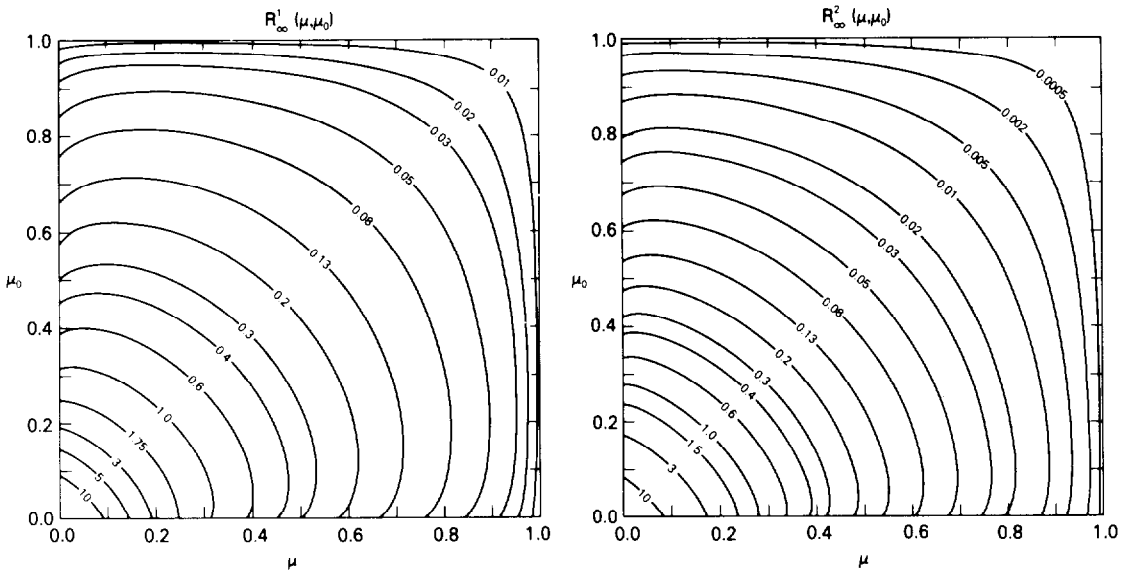

Fig. 9. Azimuth-dependent reflection functions $R_\infty^m(\mu, \mu_0)$ for $m = 1$–2 and for the Henyey-Greenstein model.

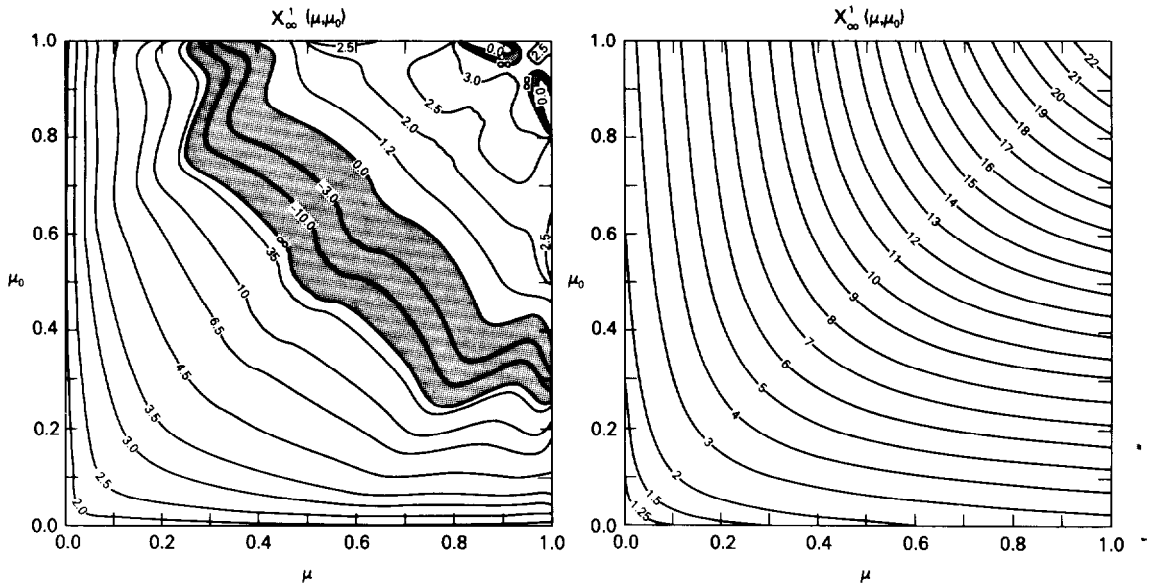

Fig. 10. Ratio of the total reflection function to the first-order reflection function $X_\infty^m(\mu, \mu_0)$ for $m = 1$. where the figure on the left applies to the FWC model and the figure on the right to the Henyey–Greenstein model.

Greenstein model having $g = 0.5$, a case for which $X_\infty^3(0.5, 0.5) = 1.272$. From these results, together with those presented by van de Hulst[6] as a function of τ_c and ω_0, we conclude that the azimuth-dependent enhancement factors for reflection increase with increasing g, increasing τ_c, and increasing ω_0. For a conservatively scattering, optically thick, atmosphere having a large asymmetry factor, the approach of $R_\infty^m(\mu, \mu_0)$ to a first-order reflection function as m increases is so slow as to be of little help in reducing the labor involved in making multiple scattering computations.

For the FWC model, illustrated in the left portion of Fig. 10, the ratio of the total reflection function to the first-order reflection function for the $m = 1$ term shows large regions where $X_\infty^1(\mu, \mu_0) < 0$, as well as angular combinations where $X_\infty^1(\mu, \mu_0) = \infty$. Comparing the distribution of positive and negative values of $R_\infty^1(\mu, \mu_0)$ with $h^1(-\mu, \mu_0)$, presented in Figs. 8 and 4, respectively, one sees that the shift in the angular position where these functions are zero accounts for the distribution of positive and negative values of $X_\infty^1(\mu, \mu_0)$. At angular positions where $R_\infty^1(\mu, \mu_0) = 0$ it is necessary that $X_\infty^1(\mu, \mu_0)$ equals zero, whereas $X_\infty^1(\mu, \mu_0)$ equals infinity when $h^1(-\mu, \mu_0)$ equals zero. The large negative region in $X_\infty^1(\mu, \mu_0)$ arises from positive values of $R_\infty^1(\mu, \mu_0)$ and negative values of $h^1(-\mu, \mu_0)$, whereas the small negative regions arise from negative values of $R_\infty^1(\mu, \mu_0)$ and positive values of $h^1(-\mu, \mu_0)$. As m increases the demarcation between positive and negative values of $R_\infty^m(\mu, \mu_0)$ increasingly coincides with angular positions where $h^m(-\mu, \mu_0)$ equals zero. As a consequence the negative regions in $X_\infty^m(\mu, \mu_0)$ become narrower as m increases, but the negative regions and singularities persist even at $m = 30$. It is therefore difficult to uniformly replace multiple scattering computations with single scattering computations as m increases for a general asymmetric phase function.

6. NUMBER OF FOURIER TERMS REQUIRED

The number of terms required in the Fourier expansion of the reflection function to achieve a given level of accuracy depends strongly on μ, μ_0 and τ_c. Restricting our attention to optically thick atmospheres, cases for which Eqs. (24)–(26) apply, it follows that Eq. (26) may be rewritten by replacing the fixed upper limit L by a variable upper limit $M(\mu, \mu_0)$ such that

$$R_\infty(\mu, \mu_0, \phi) = R_\infty^0(\mu, \mu_0) + 2 \sum_{m=1}^{M(\mu, \mu_0)} R_\infty^m(\mu, \mu_0) \cos m\phi. \tag{30}$$

When μ_0 and μ are both near grazing incidence and reflection and single scattering dominates,

$M(\mu, \mu_0)$ necessarily approaches L. On the other hand the azimuthally independent term is the only term required when either $\mu = 1$ or $\mu_0 = 1$.

The observation that $M(\mu, \mu_0)$ is a strong function of μ and μ_0 led Dave and Gazdag[2] and Hansen and Pollack[4] to suggest that multiple scattering computations could be made less time consuming by terminating the calculations at some value of m which depends on μ and μ_0. In addition to the angles of incidence and reflection, however, the values of $M(\mu, \mu_0)$ depend on the single scattering albedo and phase function as well as on the criterion used to terminate the series. As a consequence it is not in general possible to estimate *a priori* the number of azimuthal terms to be carried in the computations, except for the trival case when either $\mu = 1$ or $\mu_0 = 1$.

Figure 11 illustrates the separate terms in the Fourier expansion of the reflection function as a function of m for $\mu_0 = 0.5$ and for selected values of μ. Filled symbols indicate positive values while open symbols indicate negative values. For the Henyey–Greenstein model, presented in the right portion of Fig. 11, the azimuth-dependent reflection functions are all positive. Furthermore, the decrease of $R_\infty{}^m(\mu, \mu_0)$ with increasing m is nearly linear on a semi-logarithmic scale for $m \geq 2$, as noted by van de Hulst,[6] with the steepness of the decrease being directly related to the steepness of the angles of incidence and reflection. For a fixed angle of incidence the fewest number of azimuthal terms are required for reflection to zenith ($\mu = 1$) while the largest number of terms are required for grazing reflection ($\mu = 0$).

For the FWC model, presented in the left portion of Fig. 11, the azimuth-dependent reflection functions contain both positive and negative values (see Fig. 8). In addition, the absolute values of $R_\infty{}^m(\mu, \mu_0)$ undergo oscillations as a function of m which are not present in atmospheres obeying the Henyey–Greenstein phase function. As a consequence, the number of Fourier terms required to describe the reflection function to a given level of accuracy depends on the criterion used to terminate the series.

In the case of the fair weather cumulus model, the number of terms required to attain a relative accuracy of 0.1% can best be assessed by evaluating $R_\infty(\mu, \mu_0, \phi)$ as a function of the largest term retained in the Fourier series expansion. Figure 12 illustrates this Fourier series

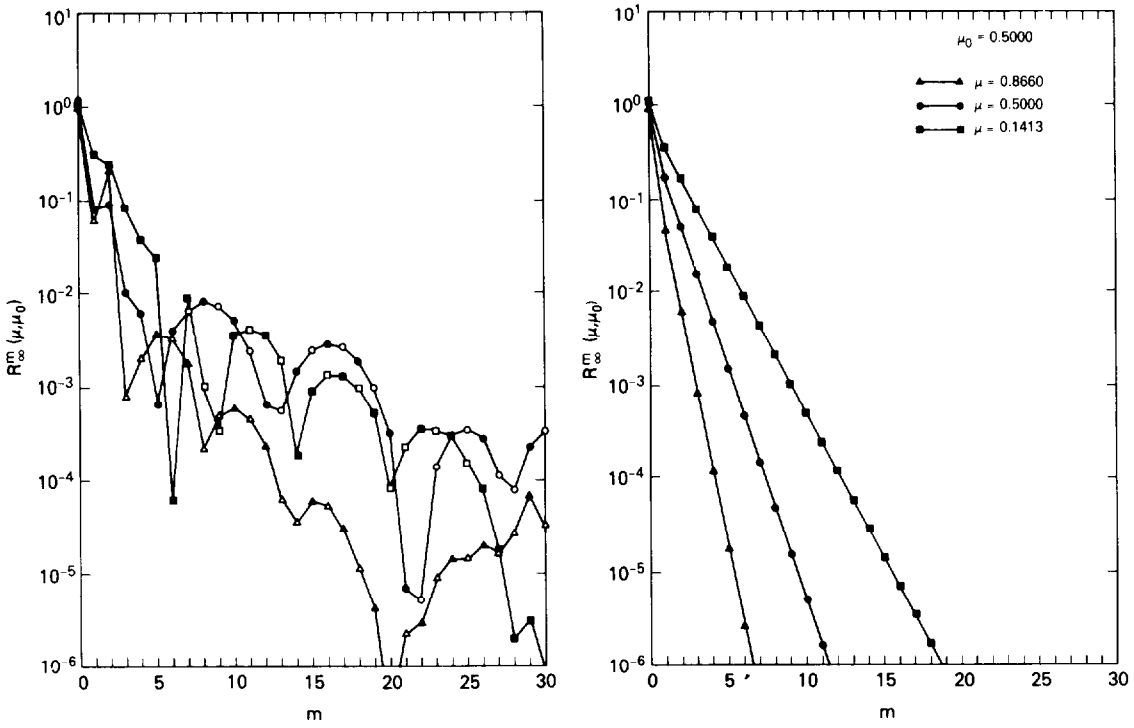

Fig. 11. Separate terms in the Fourier expansion of the reflection function of a semi-infinite atmosphere for $\mu_0 = 0.5$ and for selected values of μ. Filled symbols indicate positive values while open symbols indicate negative values. The figure on the left applies to the FWC model and the figure on the right to the Henyey–Greenstein model.

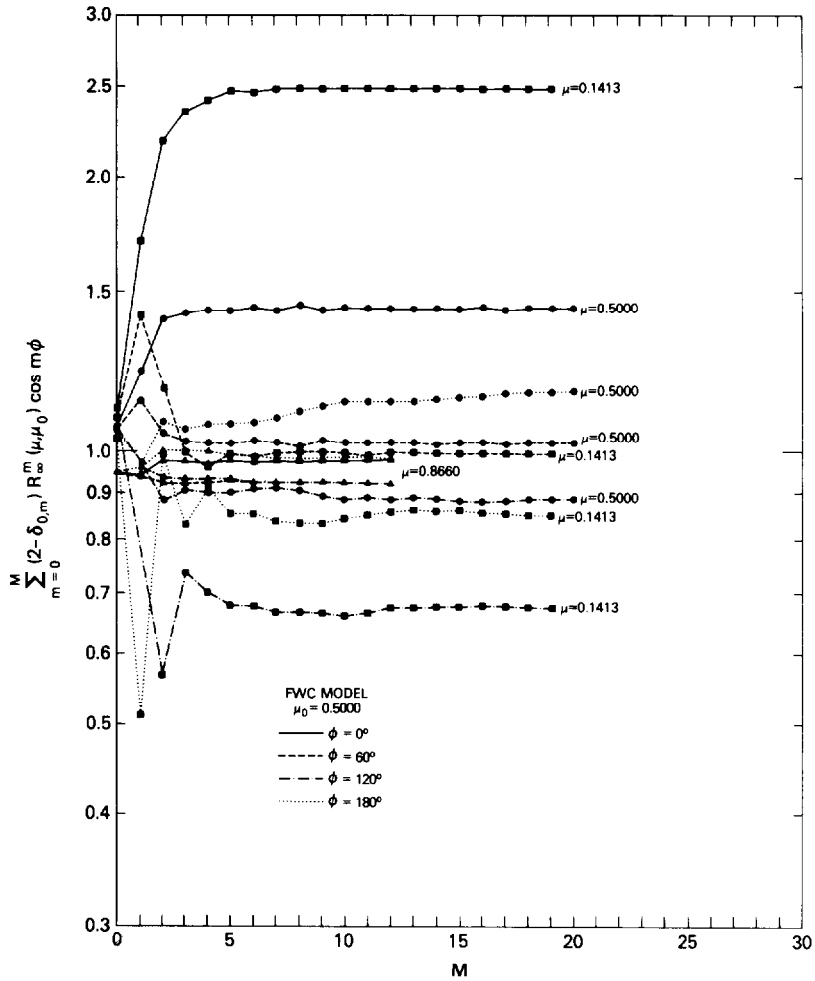

Fig. 12. Reflection function $R_\infty(\mu, \mu_0, \phi)$ as a function of the largest term retained in the Fourier series expansion of the reflection function for $\mu_0 = 0.5$ and for selected values of μ and ϕ. Results apply to the FWC model.

reconstruction for $\mu_0 = 0.5$ and for selected values of μ and ϕ. For each combination of μ and μ_0 the values of $R_\infty(\mu, \mu_0, \phi)$ which would be obtained if $M(\mu, \mu_0) = L$ were estimated for each of four azimuthal angles. Having determined estimates of $R_\infty(\mu, \mu_0, \phi)$ at selected values of ϕ, we determined values of the largest term required in the series to be assured an accuracy of 0.1%. These results were intercompared for each azimuth angle to determine a representative value for $M(\mu, \mu_0)$. As μ and μ_0 depart further from unity the inter-azimuth variability in the required number of Fourier terms tends to increase. Thus the selection of a representative value for $M(\mu, \mu_0)$ contains some subjectivity. In the results presented below the values for the required number of terms should be read give or take a few terms, with generally less terms required for azimuth angles 0° and 60° and more terms required for azimuth angles 120° and 180°. Furthermore, as the required number of terms increases it becomes increasingly more difficult to estimate asymptotic values for $R_\infty(\mu, \mu_0, \phi)$ since multiple scattering calculations were performed only out to $m = 30$. As a consequence, values of $M(\mu, \mu_0)$ are reported out to a maximum value of 23.

This description of the criterion used to terminate the Fourier series representation of the reflection function may be made more concrete by examining in detail the results presented in Fig. 12. The curves marked with the circles approach within 0.1% of their asymptotic values for all four azimuth angles at $M(\mu, \mu_0) = 19$. In this example, corresponding to the case when $\mu = \mu_0 = 0.5$, the $\phi = 0°$ and 60° azimuth planes are characterized by oscillations about asymp-

totic values of $R_\infty(\mu, \mu_0, \phi)$ for values of M less than 19, though the magnitudes of the oscillations exceed 0.1% in both cases. In the case of the $\phi = 120°$ and 180° azimuth planes more terms are required to approach asymptotic values of $R_\infty(\mu, \mu_0, \phi)$ but once approached the amplitudes of the oscillations are within the desired threshold level of 0.1%. Similarly, we find on examination of Fig. 12 that the Fourier series representation of the reflection function may be terminated at $M(\mu, \mu_0) = 18$ for $\mu = 0.1413$ and $M(\mu, \mu_0) = 11$ for $\mu = 0.8660$. Comparing these results with the magnitude of the azimuth-dependent reflection functions presented in the left portion of Fig. 11, we find that somewhat different results are obtained than might have been had we based our selection criterion solely on the amplitude of the Fourier coefficients.

Using the specified selection criterion, the number of terms required in the Fourier expansion of the reflection function was determined for the FWC model and for each value of μ and μ_0. These results, presented in the left portion of Fig. 13, yield the surprising result that for most values of μ_0 the largest number of Fourier terms are required when $\mu = \mu_0$, with generally fewer terms required when μ is either smaller or larger than μ_0. The local maximum in the vicinity $\mu = \mu_0 \sim 0.95$ is associated with angles for which the azimuthal variation of the reflection function contains multiple scattering signatures associated with the rainbow ($\phi = 0°$) and glory ($\phi = 180°$). The results presented in Fig. 13 confirm the expectations of Dave and Gazdag[2] and Hansen and Pollack[4] that multiple scattering calculations need be performed for fewer azimuthal terms than required to expand the phase function in Legendre polynomials. In the FWC model, for example, $L = 229$ and yet it is sufficient to perform multiple scattering calculations out to $m = 20$, provided one is interested in applications for which either μ or μ_0 is greater than about 0.42. For less anisotropic phase functions arising from distributions containing either smaller particles or absorbing particles, it is likely that 21 terms would be sufficient for even a larger range of μ and μ_0 values.

For the Henyey–Greenstein model the criterion used to terminate the Fourier series was that $M(\mu, \mu_0)$ be that value of m such that all $R_\infty^m(\mu, \mu_0)$ with $m > M(\mu, \mu_0)$ be less than 10^{-3} times $R_\infty^0(\mu, \mu_0)$. This criterion was adequate for the Henyey–Greenstein model due to the simple monotonically decreasing behavior of the azimuth-dependent reflection functions (see Fig. 11). These results, presented in the right portion of Fig. 13, conform with the commonly held belief that for a given value of μ_0 the number of terms required to attain a given level of accuracy monotonically increases as μ decreases. Furthermore, fewer terms are required for the Henyey–Greenstein model than for the FWC model at all values of μ and μ_0. For many aircraft and satellite applications involving scanner instruments restricted to scan angles from 0°

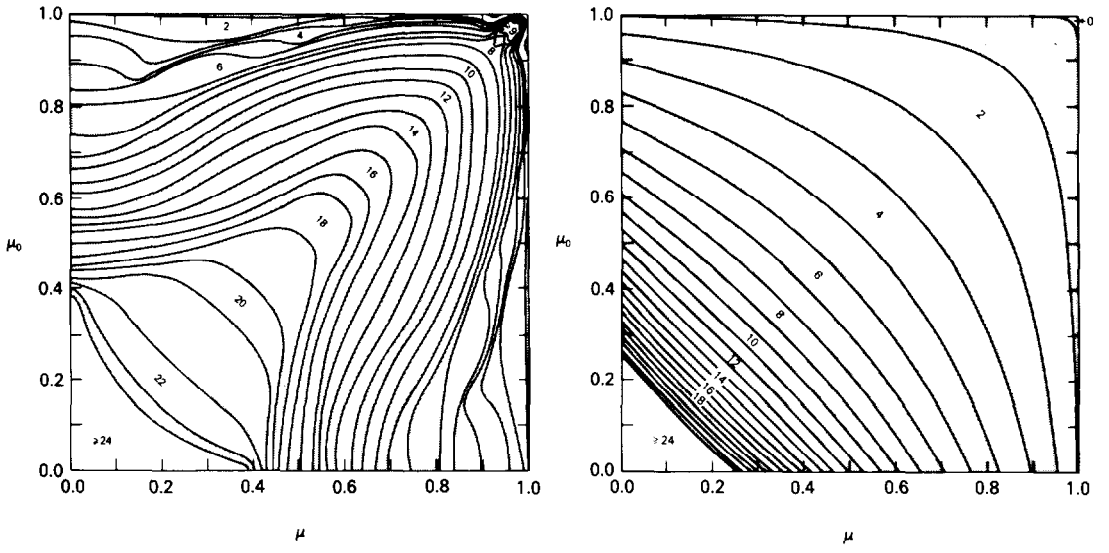

Fig. 13. Index of largest term required in the Fourier expansion of the reflection function of a semi-infinite atmosphere, where the figure on the left applies to the FWC model and the figure on the right to the Henyey–Greenstein model.

to 45°, the number of azimuthal terms required to describe the reflected intensity field for optically thick atmospheres will generally not exceed 16 ($m = 15$).

7. CONCLUSIONS

In the foregoing sections, results have been presented for the separate terms in the Fourier expansion of the reflection function of a semi-infinite, conservatively scattering, atmosphere composed of cloud particles. These results have been compared with those for an atmosphere having a Henyey–Greenstein phase function with the same asymmetry factor as in the cloud model. The relative difference in the azimuthally independent reflection function, though generally less than a few per cent, can be as large as 70% at angles where single scattering is important (*viz.*, $\mu = \mu_0 \sim 0$). The moments (plane albedo, escape function) and bimoments (spherical albedo, extrapolation length) of the azimuthally independent reflection function are generally similar for both models, whereas the azimuth-dependent terms of the reflection function are generally dissimilar. These results emphasize the fact that the similarity relations discussed by van de Hulst[6] and King[23] are the most applicable for the integrated quantities such as the spherical albedo and the least applicable for details of the reflected intensity as a function of azimuth angle.

As a prelude to performing multiple scattering calculations it is necessary that each term in the Fourier expansion of the phase function satisfy a normalization condition in quadraturized form. Though this requirement has long been recognized for the azimuth-independent term,[17] quadraturized normalization conditions for the azimuth-dependent terms are presented here for the first time. A criterion has been introduced whereby the order of the angular discretization can be estimated as a function of the number of terms required to expand the phase function in a Legendre series. Using this criterion the azimuth-dependent normalization conditions are sufficiently well satisfied that accurate intensities as well as accurate flux densities result from multiple scattering computations.

The intego-differential equations satisfied by the reflection and transmission functions, known as the principles of invariance, were solved for an optically thin initial layer by a second order Runge–Kutta method. This initialization method, which we have referred to as invariant imbedding, permits doubling computations to be initiated at a larger optical thickness than required for the single scattering initialization, with little increase in the time required to perform the initialization. Though our derivation from the principles of invariance is new, the resulting expressions for the reflection and transmission functions are entirely equivalent to Wiscombe's[16] expanded diamond initialization, once allowance is made for differences in the definition of his reflection and transmission operator's. In applications involving highly anisotropic phase functions, cases for which a large order of angular discretization is required, the invariant imbedding initialization presented here is especially attractive. Under these conditions the more accurate fourth order Runge–Kutta[21] and diamond[16] initializations require more computer time to initialize than is saved by reducing the number of doublings required.

The azimuth-dependent reflection functions of a semi-infinite atmosphere were obtained for both the fair weather cumulus and Henyey–Greenstein models by successive applications of the invariant imbedding, doubling and asymptotic fitting methods. One important finding of the present investigation is that the reflection function of a semi-infinite atmosphere can be represented by a Fourier series whose upper limit depends strongly on the angles of incidence and scattering. These results, presented in Fig. 13, show that the number of terms required to describe the reflection function is larger for a Mie theory phase function than for a Henyey–Greenstein phase function. Furthermore, the Henyey–Greenstein results show that for a fixed solar zenith angle the required number of terms increases monotonically as the zenith angle increases from 0° to 90°. On the other hand, the FWC model generally requires more terms when $\mu = \mu_0$ than when μ is either smaller or larger than μ_0. For aircraft or satellite applications involving scanning radiometers for measuring the reflected intensity field at nadir angles from 0° to 45°, the number of terms required in the Fourier expansion of the reflection function for semi-infinite atmospheres will generally not exceed 16 ($m = 15$).

For atmospheres of sufficient optical thickness that asymptotic expressions for the reflection and transmission functions apply [$(1-g)\tau_c \gtrsim 1.2$], it is only the azimuthally independent reflection function which varies with optical thickness. As a consequence, the magnitude of the

$m = 0$ terms in Fig. 11 will decrease with decreasing optical thickness whereas the $m > 0$ terms will remain unchanged. Thus in order to maintain a relative accuracy of 0.1% in the reflection function of optically thick atmospheres, more terms may be required in the Fourier series expansion of the reflection function than required for a semi-infinite atmosphere.

Acknowledgements—The author is grateful to H. G. Meyer and K. Govindaraju for aid in performing the computations.

REFERENCES

1. J. V. Dave, *Appl. Opt.* **9**, 1888 (1970).
2. J. V. Dave and J. Gazdag, *Appl. Opt.* **9**, 1457 (1970).
3. B. M. Herman and S. R. Browning, *J. Atmos. Sci.* **32**, 1430 (1975).
4. J. E. Hansen and J. B. Pollack, *J. Atmos. Sci.* **27**, 265 (1970).
5. J. E. Hansen and L. D. Travis, *Space Sci. Rev.* **16**, 527 (1974).
6. H. C. van de Hulst, *Multiple Light Scattering. Tables, Formulas, and Applications*, Vols. 1 and 2. Academic Press, New York (1980).
7. L. C. Henyey and J. L. Greenstein, *Astrophys. J.* **93**, 70 (1941).
8. J. E. Hansen, *J. Atmos. Sci.* **28**, 1400 (1971).
9. G. W. Kattawar, S. J. Hitzfelder, and J. Binstock, *J. Atmos. Sci.* **30**, 289 (1973).
10. G. W. Kattawar, *JQSRT* **15**, 839 (1975).
11. A. H. Stroud and D. Secrest, *Gaussian Quadrature Formulas*. Prentice-Hall, Englewood Cliffs, New Jersey (1966).
12. G. E. Hunt, *JQSRT* **10**, 857 (1970).
13. W. J. Wiscombe, *J. Atmos. Sci.* **34**, 1408 (1977).
14. S. Chandrasekhar, *Radiative Transfer*. Oxford University Press, Oxford (1950).
15. J. V. Dave and B. H. Armstrong, *JQSRT* **10**, 557 (1970).
16. W. J. Wiscombe, *JQSRT* **16**, 637 (1976).
17. S. Twomey, H. Jacobowitz, and H. B. Howell, *J. Atmos. Sci.* **23**, 289 (1966).
18. G. N. Plass, G. W. Kattawar, and F. E. Catchings, *Appl. Opt.* **12**, 314 (1973).
19. K. N. Liou, *An Introduction to Atmospheric Radiation*. Academic Press, New York (1980).
20. P. J. Davis and I. Polonsky, In: *Handbook of Mathematical Functions with Formulas, Graphs, and Mathematical Tables* (Edited by M. Abramowitz and I. A. Stegun). National Bureau of Standards Applied Mathematics Series No. 55, Washington, D.C. (1964).
21. G. W. Kattawar and G. N. Plass, *JQSRT* **13**, 1065 (1973).
22. W. J. Wiscombe, *JQSRT* **18**, 245 (1977).
23. M. D. King, *J. Atmos. Sci.* **38**, 2031 (1981).
24. H. C. van de Hulst, *J. Comput. Phys.* **3**, 291 (1968).
25. H. C. van de Hulst, *JQSRT* **11**, 785 (1971).